International Refereed Journal of Engineering and Science (IRJES)
ISSN (Online) 2319-183X, (Print) 2319-1821
Volume 7, Issue 4 Ver. I (April 2018), PP. 04-14

A Low Rating Photovoltaic Fed Dstatcom for Harmonic Elimination and Power Factor Correction under Non-Sinusoidal Source

Dr. A.K. Baliarsingh, D. Mishra, M. Mantri, Dr. S. Mishra
Faculty members of Electrical Engg. Department, OEC, Bhubaneswar
** Corresponding author: Dr. A.K. Baliarsingh*

ABSTRACT: This paper proposes a photovoltaic fed improved hybrid DSTATCOM for harmonic and reactive power compensation. The solar system is connected to the grid using a LCL passive filter with a series connected capacitor at the front end of voltage source inverter. The series capacitor helps in reducing the dc link voltage leading the reduction in the rating of DSTATCOM and so as also the solar system. The system is modelled and controlled by considering the non-linearity of the system. The Fuzzy logic controller is used to control the power flow from solar system and to maintain dc link voltage. To accomplish the arrangement robust, switching pulses for inverter is generated using sliding approach controller.Using Simulink, the behavior of the controllers for DC bus voltage and current control are investigated.

Date of Submission: 23-03-2018 Date of acceptance: 07-04-2018

I. INTRODUCTION

The demand to supply ratio of energy has drastically decreased due to heavy population growth and high demand electrical energy by the consumers. This is the important reason where the conventional energy sources throughout the world continue to deplete. Rapid advancement in technologies has forced the era to depend on the renewable energy sources to the grid as conventional power sources are losing their capability and sustainability to fulfil the demand to supply ratio [1]. Out of different renewable sources, the photovoltaic (PV) source becomes the eye candy for power researchers due to its abundant availability, low running cost, and along with that it has the advantage of connecting it in series to get the required dc voltage level. Through solar inverters the PV systems are generally integrated to grid. The grid connected PV system either fulfils the load active power demand or injects power to the grid. This operation of solar system can be continued till the solar radiation is sufficient for the PV system to generate active power. So during insufficient solar radiation the solar inverter remains unused [2], [3]. Considering this issue for increased utilization and efficiency, the solar invertersare also utilized to solve power quality issues caused by non-linear load [4], [5].

Power quality Issues arise due to the presence of harmonics caused by the non-linear load which affects the performance in terms of voltage distortion, harmonics and power factor. Use of the conventional ways to solve the issues related to the power quality by implementation of the passive filters, creates problems likeresonance, fixed compensation, heavy weightand large space requirement which make the system operation more complex and faulty [6-7]. Considering the issues related to the conventional filters researchers introduced power quality improvement devices like distribution static compensators (DSTATCOMs) having capability to provide the compensation for changing harmonics,reactive power, and unbalanced source currents [8-9]. Now these DSTACOMs are integrating with solar system (named as PV-DSTATCOMs) for combined operation of integration to grid and power quality enhancement [10-14].

The PV-DSTACOMs are integrated to grid through voltage source inverters and passive filters like L or LCL switching harmonic minimizing filter. A large drop across the inductance of conventional Lswitching harmonic minimizing filterforces for higher dc link voltage and as well as increased VSI weight, cost and power rating. To avoid the limitations of traditional L filter, hybrid LCL filters are proposed in [13]. Different control techniques are applied to enhance the compensator performance [15-24]. In [10] a new hybrid topology for DSTATCOM is proposed, in which a capacitor in connected in series with LCL filter at the front end of voltage source inverter to overcome the problems LCL filter and a damping resistor is connected in series with shunt capacitor of LCL filter to avoid resonance damping. The author had shown that with proposed topology the power rating of DSTATCOM had been reduced without affecting the compensation capability of the compensator.

In this paper, a new PV-DSTATCOM topology is proposed which operates at lower power rating. With the proposed topology comparatively smaller photovoltaic source can also be integrated to grid without boost

converter. For current control the performance of the system is observed and compared with two different controller named as modified instantaneous $i_d - i_q$ theory and sliding mode control (SMC). Similarly for dc bus voltage control two techniques are applied, one is proportional plus integral (PI) controller and the other one is Fuzzy logic controller. The efficacy of the proposed topology is verified through both simulation and experimental results.

The paper is organized as follows. Section 2 presents the brief discussion about proposed topology and its effect on real power flow from solar system. It also discuss the non-linear modelling of PV-DSTATCOM. The design of different current controllers and voltage controllers are described in section 3. Section 4 presents the simulation results and discussions. The experimental results are presented in section 5 and section 6 concludes the paper.

II. OUTLINE OF PV FED HYBRID DSTATCOM

The photovoltaic fed hybrid distribution static compensator (PV-DSTATCOM) considered for studying purpose is shown in Fig. 1(A). The implemented system consists of a photovoltaic array, three phase solar inverter, a non-linear load (means three phase bridge rectifier with ohmic-inductive load) and the distribution grid. The solar inverter is integrated to grid through an LCL filter and series capacitor. The system transfers the active power from PV array when solar radiation is available and also satisfies the compensating capability of DSTATCOM. Rest of time, the implemented system behaves as a conventional DSTATCOM. As shown in Fig. 1(a), R_1 and L_1 are inverter side resistance and inductance respectively; R_2 and L_2 represents the load side resistance and inductance respectively; C_f is the LCL filter capacitance connected in shunt with all three phases; a damping resistor is connected in series with the capacitor (C_f) for passive damping of the total system represented as R_d; the series capacitor inserted in series at the front end of LCL filter is represented as C_{se}; Source impedance is represented as R_s, L_s; voltage across the dc link capacitor (C_{dc}) and the source voltage are represented as V_{pv}, and V_s respectively; V_{pa}, V_{pb}, V_{pc} represents voltage at the point of common coupling (PCC) for phase a, b, and c respectively; load currents for all phases and source current are represented as i_{la}, i_{lb}, i_{lc}, and i_s respectively. The system parameters are given in Table 1.

The dynamic model of the presented system under synchronous reference frame can be expressed as follows:

$$\frac{di_{1j}}{dt} = \frac{D_j V_{pv}}{L_1} - \frac{R_d}{L_1} i_{1j} + \frac{R_d}{L_1} i_{2j} - \frac{V_{cfj}}{L_1} \pm \omega i_{1j'} \quad (1)$$

$$\frac{di_{2j}}{dt} = \frac{R_d}{L_2} i_{1j} - \frac{R_d}{L_2} i_{2j} - \frac{V_{sej}}{L_2} - \frac{V_{sj}}{L_2} + \frac{V_{cfj}}{L_2} \pm \omega i_{2j'} \quad (2)$$

$$\frac{dV_{pv}}{dt} = \frac{1}{C_{dc}} i_{pv} - \frac{1}{C_{dc}} \left[D_d i_{1d} + D_q i_{1q} \right] \quad (3)$$

$$\frac{dV_{cfj}}{dt} = \pm \omega V_{cfj'} + \frac{1}{C_f} \left[i_{1j} - i_{2j} \right] \quad (4)$$

$$\frac{dV_{sej}}{dt} = \pm \omega V_{sej'} + \frac{1}{C_{se}} i_{2j} \quad (5)$$

where $j = d, q$, $j' = q, d$, i_{1j} and i_{2j} denote d-q axis VSI currents and filter currents respectively, V_{cfj} is the d-q axis voltage across shunt capacitor, V_{sej} represents the voltage across the series capacitor, D_j stands for d-q axis duty ratio functions. By considering the dynamic equation,the average model of the system is shown in Fig. 1(B).

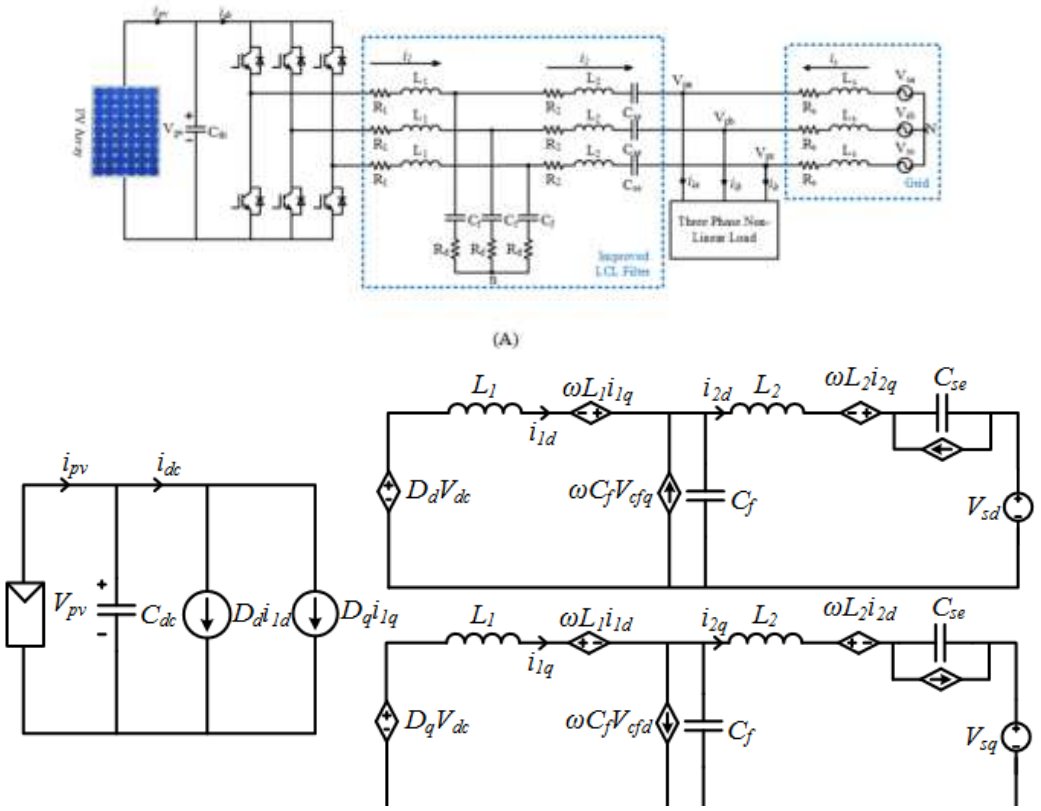

Fig. 1 (A) Line diagram of PV fed hybrid LCL filter based DSTACOM (B) Average model of implemented system

The reactive power compensation capability of the implemented system without photovoltaic source is discussed and verified in [9]. As the integration of photovoltaic source with the proposed hybrid filter will not affect

Table 1 System parameters

Parameters	Value
Grid Voltage (V_s)	230V rms
System Frequency	50Hz
DC Link Voltage(V_{pv})	165V
DC Link Capacitor (C_{dc})	3000μF
Non-linear load (3-phase diode bridge rectifier with R-L load) R_{dc}, L_{dc}	50Ω, 200mH
LCL filter parameters (L_1, C, L_2, C_{se})	1.3mH, 15μF, 0.4mH, 65μF

the reactive power compensation capability, so here only the changes in active power flow between grid, PV source and non-linear is discussed. The insertion of series capacitor caused the reduction of dc link voltage. Through a tradeoff process dc link voltage is chosen 165V which found to provide satisfactory compensation. By applying Kirchhoff's voltage law in the system, we get:

$$V_{inv}^1 - I_f^1 R_f - I_f^1 jX_{f12} - I_f^1 jX_{se}^1 - V_p^1 = 0 \quad (6)$$

where the fundamental voltage available at the VSI side (V_{inv}^1) is $\frac{V_{pv}}{\sqrt{2}}$, $R_f = R_1 + R_2$, $X_{f12} = \omega_1(L_1 + L_2)$, $X_{se1} = 1/\omega_1 C_{se}$, and V_p^1 is the fundamental pcc voltage. From(6), the real part of the fundamental current supplied by the filter can be expressed as:

$$Re\left[I_f^1\right] = \frac{R_f\left(V_{inv}^1 - V_p^1\right)}{\left(X_{f12} - X_{se}^1\right)^2} \quad (7)$$

From(7), it can be noticed that the impedance of passive filter decreased due to the insertion of series capacitor. Therefore the same active current can be injected to load through the compensator with reduced dc

link voltage and as well as with reduced output voltage of photovoltaic system. When conventional L or LCL filters are used for the interfacing of solar inverter with grid, generally the dc bus voltage required for satisfied operation of compensator is around (650-780)V. When dc bus voltage will be high, the inverter rating will increase as the power rating of the required IGBTs will be high. With increase in rating, the price per unit IGBT will also increase, which will make the inverter costlier as compared the inverter whose dc bus voltage is 165V. Again if dc link voltage will be high, then low rating PV sources (whose output open circuit voltage is low) will need a boost converter to be integrated with grid. But with the implemented system, the above discussed problems which are responsible for price hike of overall system can be avoided.

III. CONTROLLER DESIGN

In this section the control strategies for reference current generation, dc link voltage control and switching signal generation for voltage source inverter is discussed. The modified instantaneous $i_d - i_q$ theory for reference current generation, fuzzy logic control for maintaining the dc bus voltage at its reference value and sliding mode control for generation of switching pulses for inverter are implemented. The control methods used are now briefly enlightened.

4.1 Reference current generation

The reference current is generated using $i_d - i_q$ method. The load currents are sensed and Park's transform is performed to calculate the load current in dq axis. The load currents are transformed using the following matrix:

$$\begin{bmatrix} i_{Ld} \\ i_{Lq} \end{bmatrix} = \begin{bmatrix} \sin\theta & \cos\theta \\ -\cos\theta & -\sin\theta \end{bmatrix} \begin{bmatrix} 1 & -1/2 & -1/2 \\ 0 & \sqrt{3}/2 & -\sqrt{3}/2 \end{bmatrix} \begin{bmatrix} i_{La} \\ i_{Lb} \\ i_{Lc} \end{bmatrix} \quad (8)$$

For transformation, the needed transformation angle 'θ' generally obtained through phase locked loop (PLL) or a synchronizing circuit. But here the transformation angle is calculated as follows:

$$\cos\theta = \frac{V_\alpha}{\sqrt{V_\alpha^2 + V_\beta^2}} \quad (9)$$

$$\sin\theta = \frac{V_\beta}{\sqrt{V_\alpha^2 + V_\beta^2}} \quad (10)$$

$$\text{where } \begin{bmatrix} V_\alpha \\ V_\beta \end{bmatrix} = \sqrt{\frac{2}{3}} \begin{bmatrix} 1 & -1/2 & -1/2 \\ 0 & \sqrt{3}/2 & -\sqrt{3}/2 \end{bmatrix} \begin{bmatrix} V_a \\ V_b \\ V_c \end{bmatrix} \quad (11)$$

Through this way the synchronizing circuit can be avoided thus by reducing the complexity of the system.

After transformation the fundamental component and the harmonics of load current will appear as dc value and ripple respectively. The dc offset is filtered out through low pass filter and removed from the transformed signal to find out the harmonic isolated dq transformed signal. The generation of reference currents is illustrated inFig. 2 (C). Now the reference filter current is calculated as:

$$i_{2d}^* = i_{ld} - i_{sd}^*$$

$$i_{2q}^* = i_{lq} - i_{sq}^* \quad (12)$$

4.2 DC bus voltage control with Fuzzy logic controller

In this section the fuzzy logic control shown in Fig. 2 (A), is implemented for maintain the dc link voltage at its required magnitude. The dc bus controller consists offuzzy controller and limiter to generate the peak magnitude of current required for maintaining the real power flow balance between both the source and load.The sensed dc voltage is compared with the reference value and the error is given as the input to the fuzzy controller for further processing. The work flow of the fuzzy controller is characterized as seven fuzzy set rules

for each input and output, fuzzyfication, implication using Mamdani's max operator method and defuzzyfication using centroid method.

The triangular curve is a function of a vector 'X' and depends on three scalar parameters a, b and c as shown below

$$\mu_A(\mathrm{x}) = \min\left(\max\left(\frac{x-a}{b-a}, \frac{c-x}{c-b} \right), 0 \right)$$

(13)

Fuzzy controller makes the dc bus control an automated control whose functional rules are constructed basing on expert experience or knowledge base. In Fig. 2 (B) seven membership functions are used for each input (NL negative large, NM negative medium, NS negative small, ZE zero, PS positive small, PM positive medium, PL positive large). The fuzzy rules are shown in Table 2.

Table 2 Fuzzy control rules table

Δe	NB	NM	NS	Z	PS	PM	PB
e							
NB	NB	NM	NS	Z	PS	PM	PB
NM	NS	NB	NB	NM	NS	Z	PS
NS	NB	NB	NB	NB	NB	NM	NS
Z	PM	NS	Z	PS	PM	PB	PB
PS	NM	NB	NB	NB	NM	NS	Z
PM	Z	NB	NM	NS	Z	PS	PM
PB	PS	NM	NS	Z	PS	PM	PB

4.3 Design of sliding mode controller

The implemented system is expressed in terms of state space form as follows:

$$\dot{x} = f(x) + G(x)u$$

$$y = H(x)$$

(14)

where $x = [i_{1d}, i_{1q}, i_{2d}, i_{2q}, V_{cfd}, V_{cfq}, V_{sed}, V_{seq}, V_{pv}]$, $u = [D_d, D_q]^T$, $y = [i_{2d}, i_{2q}]$

The functions can be represented as

$$f(x) = \begin{bmatrix} -\frac{R_d}{L_1} i_{1d} + \frac{R_d}{L_1} i_{2d} - \frac{V_{cfd}}{L_1} + \omega i_{1q} \\ -\frac{R_d}{L_1} i_{1q} + \frac{R_d}{L_1} i_{2q} - \frac{V_{cfq}}{L_1} - \omega i_{1d} \\ \frac{R_d}{L_2} i_{1d} - \frac{R_d}{L_2} i_{2d} - \frac{V_{sed}}{L_2} - \frac{V_{sd}}{L_2} + \frac{V_{cfd}}{L_2} + \omega i_{2q} \\ \frac{R_d}{L_2} i_{1q} - \frac{R_d}{L_2} i_{2q} - \frac{V_{seq}}{L_2} - \frac{V_{sq}}{L_2} + \frac{V_{cfq}}{L_2} - \omega i_{2d} \\ \omega V_{cfq} + \frac{1}{C_f}\left[i_{1d} - i_{2d} \right] \\ -\omega V_{cfd} + \frac{1}{C_f}\left[i_{1q} - i_{2q} \right] \\ \omega V_{seq} + \frac{1}{C_{se}} i_{2d} \\ -\omega V_{sed} + \frac{1}{C_{se}} i_{2q} \\ \frac{1}{C_{dc}} i_{pv} \end{bmatrix} \quad G(x) = \begin{bmatrix} \frac{V_{pv}}{L_1} & 0 \\ 0 & \frac{V_{pv}}{L_1} \\ 0 & 0 \\ 0 & 0 \\ 0 & 0 \\ 0 & 0 \\ 0 & 0 \\ 0 & 0 \\ \frac{i_{id}}{C_{dc}} & \frac{i_{1q}}{C_{dc}} \end{bmatrix} \quad H(x) = \begin{bmatrix} i_{2d} \\ i_{2q} \end{bmatrix}$$

The mathematical expression for sliding surface is given as follows:

$$S=\begin{bmatrix} S_d \\ S_q \end{bmatrix}=\begin{bmatrix} \left(i_{2d}^{*}-i_{2d}\right)+\gamma_1\int_0^t\left(i_{2d}^{*}-i_{2d}\right)d\tau \\ \left(i_{2q}^{*}-i_{2q}\right)+\gamma_2\int_0^t\left(i_{2q}^{*}-i_{2q}\right)d\tau \end{bmatrix}$$

(15)

where γ_1 and γ_2 are 8,000,000. Once the sliding surface is chosen the control law should be derived. The system to remain in the sliding surface, the law to be satisfied is

$\dot{S}=0$

Taking above expression into consideration, (15) can be written as

$$\dot{i}_{2d}=\dot{i}_{2d}^{*}+\left(K_1+\gamma_1\right)\left(i_{2d}^{*}-i_{2d}\right)+K_2 sign(S_d) \quad (16)$$

$$\dot{i}_{2q}=\dot{i}_{2q}^{*}+\left(K_3+\gamma_2\right)\left(i_{2q}^{*}-i_{2q}\right)+K_4 sign(S_q) \quad (17)$$

Again

$$\left(i_2\right)_{d,q}=\left(i_1\right)_{d,q}-C_f\frac{d}{dt}\left(V_{cf}\right)_{d,q} \quad (18)$$

Substituting (18) into (1) and comparing it with (16) and (17), the non-linear control law can be derived as

$$D_d=\left[i_{2d}^{*}+\left(K_1+\gamma_1\right)\left(i_{2d}^{*}-i_{2d}\right)+K_2 sign(S_d)+\frac{R_d}{L_1}i_{1d}-\frac{R_d}{L_1}i_{2d}+\frac{V_{cfd}}{L_1}-\omega i_{1q}+C_f\frac{d}{dt}V_{cfd}\right]\frac{L_1}{V_{pv}}$$

(19)

$$D_q=\left[i_{2q}^{*}+\left(K_3+\gamma_2\right)\left(i_{2q}^{*}-i_{2q}\right)+K_2 sign(S_q)+\frac{R_d}{L_1}i_{1q}-\frac{R_d}{L_1}i_{2q}+\frac{V_{cfq}}{L_1}+\omega i_{1d}+C_f\frac{d}{dt}V_{cfq}\right]\frac{L_1}{V_{pv}}$$

(20)

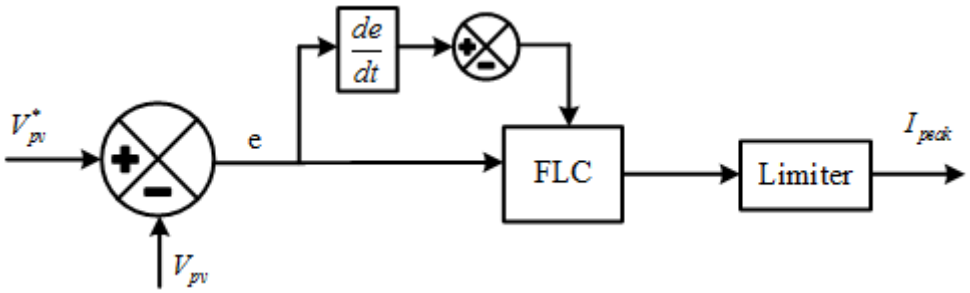

(a)

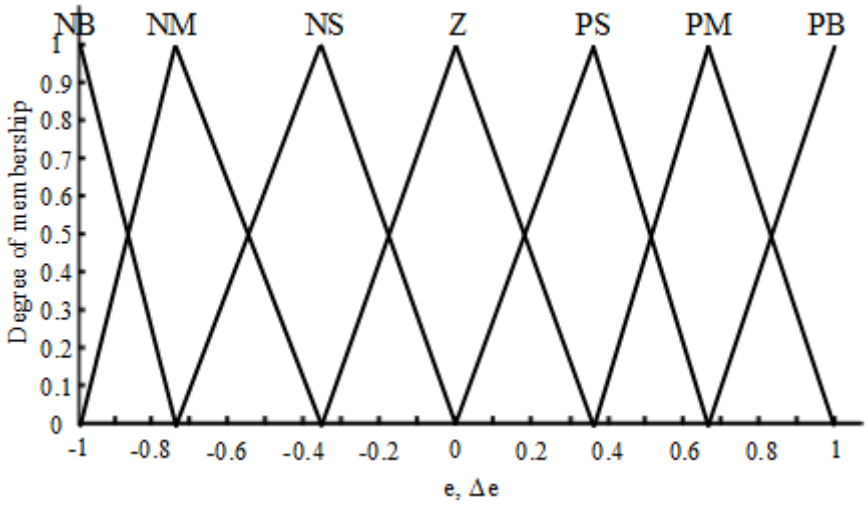

(b)

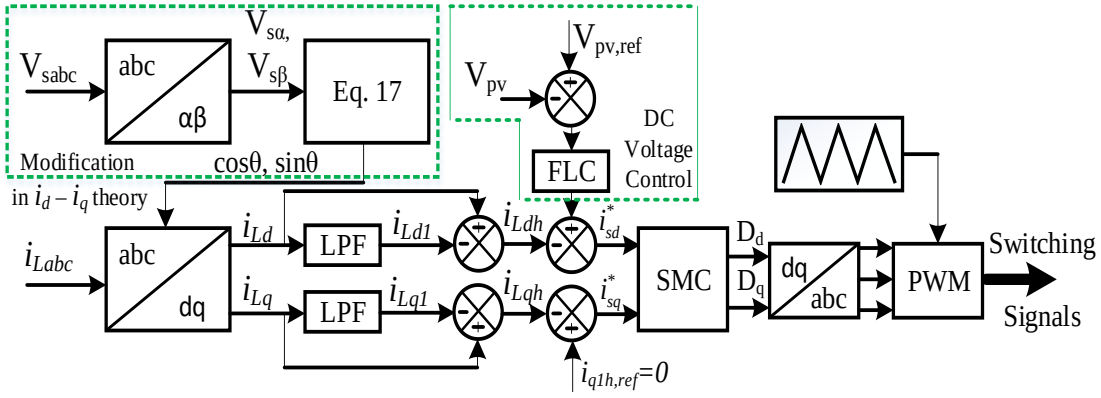

(c)

Fig. 2(a) Fuzzy inference system for dc voltage control (b) membership functions for input variables e, Δe(c) Overall implemented control structure layout

IV. SIMULATION RESULTS AND DISCUSSION

In this section the electric power system of Fig. 2 (a) is simulated. The parameters of power system and solar source are shown inTable 1and Table 3. Initially the system simulated under MATLAB/Simulink environment. The system is simulated under two different mains voltage condition. The steady state performance of the system is observed under three different control environment. The efficacy of the controllers are validated by taking total harmonic distortion, steady state error and reactive power compensation as performance index.

Table 3 KC200GT PV array parameters at nominal operating conditions

Parameters	Symbol	Value
Rated maximum power	P_{max}	200.143W
Short circuit current	I_{SC}	8.21A
Open circuit voltage	V_{OC}	32.9
Diode ideality constant	a	1.3
Series resistance	Rs	0.221Ω
Shunt resistance	Rp	415.405Ω
S.C temperature coefficient	Ki	0.0032A/K
Number of PV array in series	--	10
Number of PV array in parallel	--	2

Case-1: Steady state performance of the system with modified $i_d - i_q$ and PI controller

Under this section the power system is simulated with ideal and distorted mains voltage condition. The simulation results are shown in Fig. 3 and Fig. 4 for ideal and distorted voltage respectively. FromFig. 3, we can realize that the three phase load currents are highly distorted and non-sinusoidal due to the nonlinear load. After the compensation the source current becomes pure sinusoidal and free of distortions. But from Fig. 4 it is observed that the controller is not being capable to track the reference so proficiently as compared to the ideal mains voltage condition. Under ideal source though the controller is achieved the unit power factor requirement but under distorted source the reactive power compensation is not satisfactory. The THD of the source current reduces from 25.56% to 3.24% with ideal voltage source whereas with distorted source it reduces to 3.57% from 32.76% after compensation, which is well under the requirement of IEEE 519 standard.

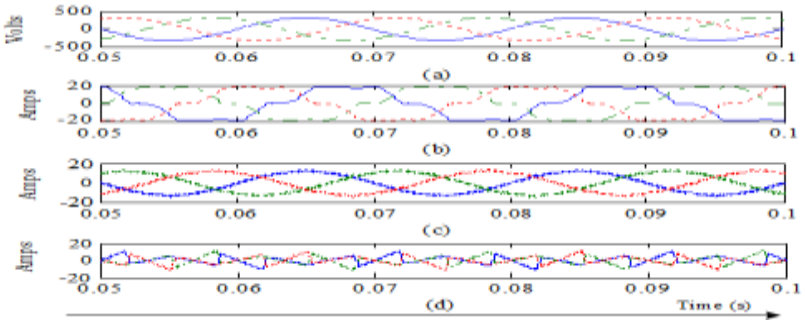

Fig. 3 Steady state performance with *modified* $i_d - i_q$ *and PI controller*(a) ideal source voltage (b) load current before compensation (c) source current after compensation (d) filter current

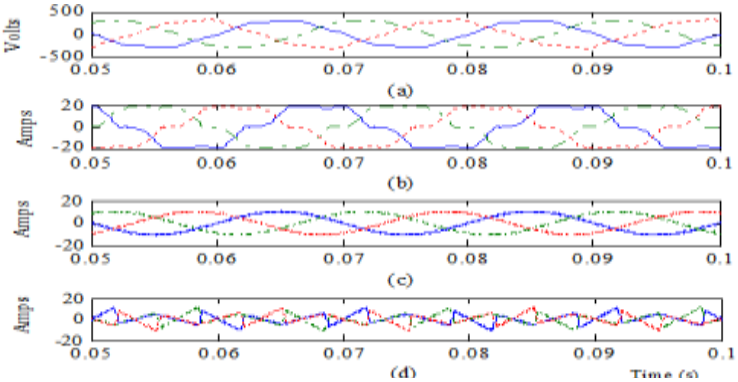

Fig. 4 Steady state performance with *modified* $i_d - i_q$ *and PI controller*(a) distorted mains voltage (b) load current before compensation (c) source current after compensation (d) filter current

Case-2: Steady state performance of the system with modified $i_d - i_q$***, PI and SMC controller***

Here the performance of the system is observed with non-linear controller named as sliding mode control (SMC). The modified instantaneous $i_d - i_q$ theory and PI controllers are used for reference current generation and dc bus voltage control. For switching pulse generation the sliding mode controller is implemented. The implementation of SMC control makes the controller robust towards any change in mains voltage or load.From Fig. 5 and Fig. 6, it is justified that the performance of the controller is satisfactory for both ideal and as well as distorted voltage source. With the proposed controller the compensator reactive power compensation as well as THD reduction capability reached to satisfactory margin.As the error minimizing capability of the controller increased due to SMC controller the noise in source current after compensation is also reduced. The THD of the source current is reduces to 2.12% for ideal source and distorted mains condition after the compensation.

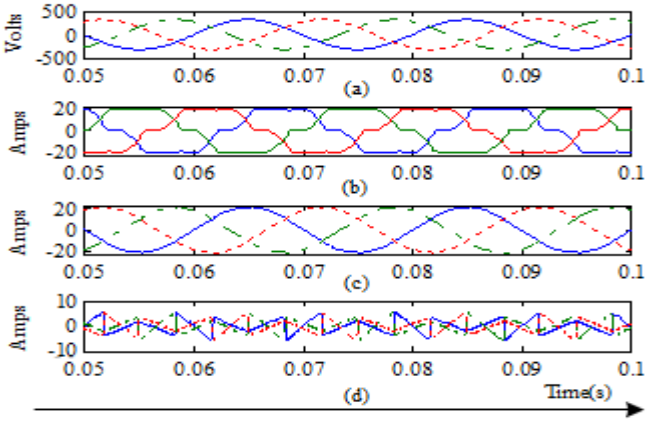

Fig. 5 Steady state performance with *modified* $i_d - i_q$ *PI and SMC controller* (a) ideal mains voltage (b) load current before compensation (c) source current after compensation (d) filter current

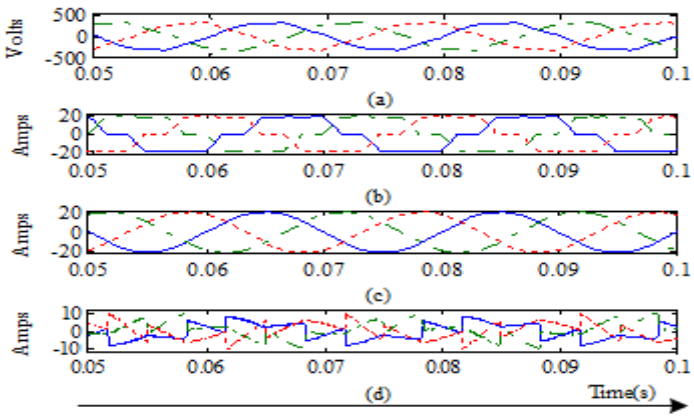

Fig. 6 Steady state performance with *modified* $i_d - i_q$ *, PI and SMC controller*(a) distorted mains voltage (b) load current before compensation (c) source current after compensation (d) filter current

Case-3: Steady state performance of the system with modified $i_d - i_q$ ***, Fuzzy and SMC controller***

Under this section, the performance of the system is evaluated with controller like modified $i_d - i_q$ theory for reference current generation, SMC controller for switching pulse generation for IGBTs and Fuzzy logic controller for dc bus voltage control. The implementation of Fuzzy controller makes the dc voltage control automated for any transient condition of the electric power system. With both Fuzzy and SMC control the total harmonic distortion of the source current after compensation reduces to 1.21% for both ideal and distorted mains condition. The steady state performance of the PV-DSTATCOM with the proposed controller is shown in Fig. 7 and Fig. 8.

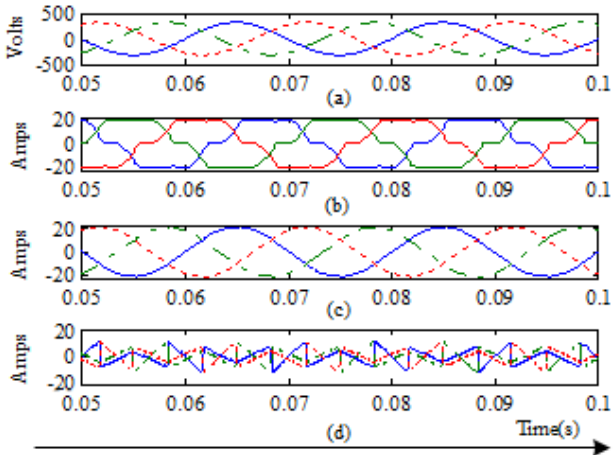

Fig. 7 Steady state performance with modified $i_d - i_q$, SMC and Fuzzy controller (a) ideal mains voltage (b) load current before compensation (c) source current after compensation (d) filter current

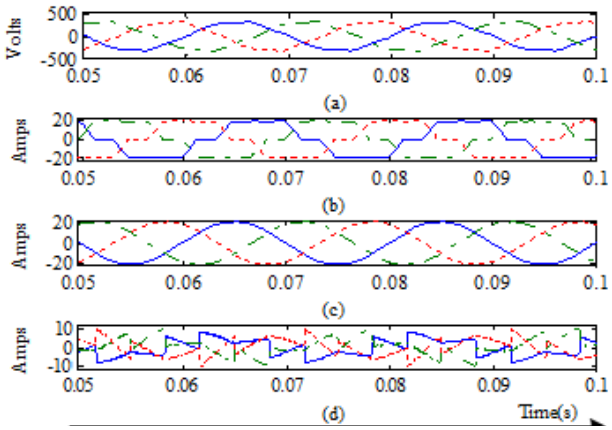

Fig. 8 Steady state performance with modified $i_d - i_q$,SMC and Fuzzy controller (a) distorted mains voltage (b) load current before compensation (c) source current after compensation (d) filter current

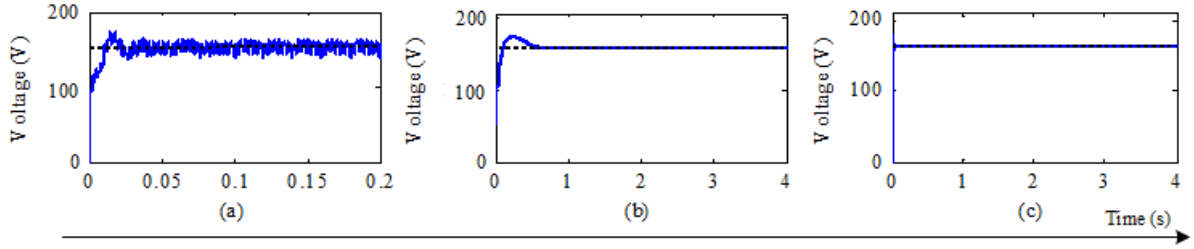

Fig. 9 DC link voltage with (a) linear controller (b) SMC controller (c) Fuzzy controller

Case-5: Transient performance with SMC under ideal source

In electrical power system the thyristorized converters are used to control the performance of the system as per the requirement. The controlled rectifier based loads are controlled by controlling the firing angle of the converter to ensure the required output. In this paper a thyristor based rectifier with ohmic-inductive load is considered for simulation. For this case the firing angle of the thyristor is varied abruptly. The system is simulated with the firing angle 30^0 till 0.1s then changed to 60^0 for 2.5 cycles. At 0.15s again the load is operated with the firing angle 30^0 for 0.05s and then operated at 90^0 firing angle at 0.2s. The load continues to operate with firing angle 30^0 after 0.25s for the rest of the simulation period. To increase the harshness of the system this condition is simulated under distorted mains voltage. From the Fig. 10, it is cleared that though the load current is more distorted and power consumption is varied, the compensator with SMC and Fuzzy controller performs satisfactorily. The THD of the source current after compensation is found to be reduced to1.45% from 40.67%.

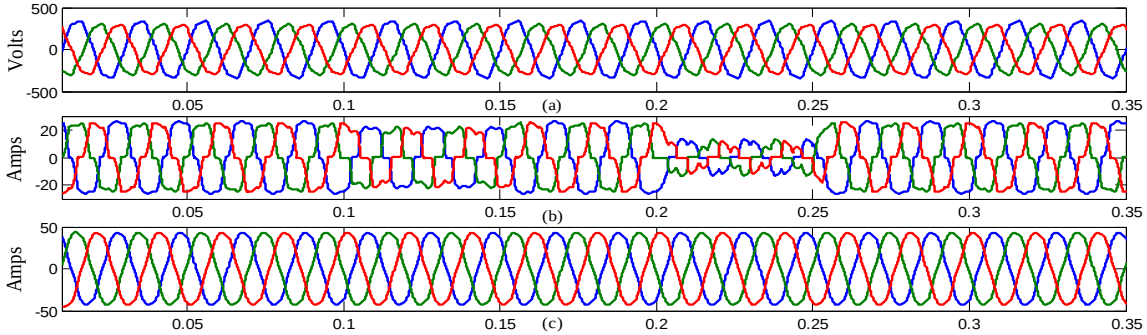

Fig. 10 Transient performance with SMC and Fuzzy controller (a) Distorted source voltage (b) load current before compensation (c) source current after compensation

V. CONCLUSION

In this paper, the modified instantaneous $i_d - i_q$ theory with PI control, SMC based $i_d - i_q$ control and Fuzzy control are surveyed. For current control, linear $i_d - i_q$ as well as nonlinear SMC based control are

implemented and the behavior of the compensator was investigated. From the investigation it was concluded that SMC control gives better performance than linear control for distorted supply conditions. Similarly for dc bus voltage control, PI controller and Fuzzy logic controller are applied. The ability of Fuzzy controlled inverter for uninterrupted compensation of reactive power of the load was studied.

REFERENCES

[1]. J. C. Schaefer, "Review of photovoltaic power plant performance andeconomics," IEEE Trans. Energy Convers., vol. 5, no. 2, pp. 232–238,Jun. 1990.

[2]. R. Noroozian and G. B. Gharehpetian, "An investigation on combined operation of active power filter with photovoltaic arrays," Electrical Power and Energy Systems, vol. 46, pp. 392-399, 2013.

[3]. G. Tsengenes and G. Adamidis, "Investigation of the behavior of a three phase grid connected photovoltaic system to control active and reactive power," Electric Power Systems Research, vol. 81, pp. 177-184, 2011.

[4]. J. He, Y. Wei Li, and M. Munir, "A Flexible Harmonic Control Approach Through Voltage-Controlled DG–Grid InterfacingConverters," IEEE Trans. Ind. Electron., vol. 59, no. 1, pp. 444-455, Jan. 2012.

[5]. M. S. Munir and Y. W. Li, "Residential distribution system harmonic compensation using PV interfacing inverter," IEEE Transaction on Smart Grid, vol. 4, no. 2, pp. 816-827, 2013.

[6]. Ghosh and G. Ledwich, Power Quality Enhancement Using Custom Power Devices, Kluwer Academic Publishers, 2002.

[7]. Singh, B., AI-Haddad, K., and Chandra, A.: 'A review of active filtersfor power quality improvement', IEEE Trans. Ind Electron., 1999, 46, (5), pp. 960-971.

[8]. B. Singh, P. Jayaprakash, D. P. Kothari, A. Chandra and K. A. Haddad, "Comprehensive Study of DSTATCOM Configurations," IEEE Trans. on Industrial Informatics, vol. 10, no. 2, pp. 854-870, May 2014.

[9]. W. N. Chang and K. D. Yeh, "Design and Implementation of DSTATCOM with symmetrical components method for fast load compensation of unbalanced distribution systems," Proc. of IEEE Power Electronics and Drive Systems Conf., vol. 2, pp. 13-20, 2003.

[10]. C. Kumar and M. K. Mishra, "An improved hybrid DSTATCOM topology to compensate reactive and nonlinear loads," IEEE Transaction on Industrial Electronics, vol. 61, no. 12, pp. 6517-6527, 2014.

[11]. K. Kannan and N. Rengarajan, "Photovoltaic based distribution static compensator for power quality improvement," Electrical Power and Energy Systems, vol. 42, no. 1, p. 685–692, 2012.

[12]. V. K. Kannan and N. Rengarajan, "Investigating the performance of photovoltaic based DSTATCOM using I cos Φ algorithm," Electrical Power and Energy Systems, vol. 54, p. 376–386, 2014.

[13]. Y. A. -R. I. Mohamed, "Mitigation of dynamic, unbalanced, and harmonic voltage disturbances using grid-connected inverters with LCL filter," IEEE Transactions on Industrial Electronics, vol. 58, no. 9, pp. 3914-3924, 2011.

[14]. J. He, Y. Wei Li, and M. Munir, "A Flexible Harmonic ControlApproach Through Voltage-Controlled DG–Grid Interfacing Converters," IEEE Trans. Ind. Electron., vol. 59, no. 1, pp. 444-455, Jan. 2012.

[15]. W. Libo, Z. Zhengming, and L. Jianzheng, "A Single-Stage Three-PhaseGrid-Connected Photovoltaic System With Modified MPPT Method andReactive Power Compensation," IEEE Trans. Energy Conv., vol. 22, no.4, pp. 881-886, Dec. 2007.

[16]. X. Wang, F. Zhuo, J. Li, L. Wang, and S. Ni, "Modeling and Control of Dual-Stage High-Power Multifunctional PV System in d-q-o Coordinate," IEEE Trans. Ind. Electron., vol. 60, no. 4, pp. 1556-1570, Apr. 2013.

[17]. V. Khadkikar, R.Varma, R. Seethapathy, A. Chandra, Hatem Zeineldin, Impact of Distributed Generation Penetration on Grid Current Harmonics Considering Non-linear Loads"," in Proc. 2012 3rd Int. Symp PEDG, pp. 608-614, Jun 25-28, 2012.

[18]. H. Akagi, Y. Kanazawa and A. Nabae , "Generaized theory of instantaneous reactive power in three phase circuits," In conf. Rec. IEEE/APEC, pp. 625-630, 1984.

[19]. T. Zaveri, B. Bhalja and N. Zaveri, "Comparison of control strategies for DSTATCOM in three-phase, four-wire distribution system for power quality improvement under various source voltage and load conditions," Electrical Power & Energy Systems, vol. 43, no. 1, p. 582–594, 2012.

[20]. B. Singh and S. R. Arya, "Back-Propagation Control Algorithm for Power Quality Improvement Using DSTATCOM," IEEE Transactions on Industrial Electronics, vol. 61, no. 3, pp. 1204 - 1212, 2014.

[21]. B. Singh, P. Jayaprakash, S. Kumar and D. P. Kothari, "Implementation of Neural-Network-Controlled Three-Leg VSC and a Transformer as Three-Phase Four-Wire DSTATCOM," IEEE Transactions on Industry Applications, vol. 47, no. 4, pp. 1892 - 1901, 2011.

[22]. A. Ghamri, M. T. Benchouia and A. Golea, "Sliding mode control based three phase shunt active power filter: Simulation and Experimentation," Electric Power Components and Systems, vol. 40, no. 4, pp. 383-398, 2012.

[23]. W. Lu, C. Li and C. Xu, "Sliding mode control of shunt hybrid active power filter based on the inverse system method," Electrical Power and Energy Systems, vol. 57, pp. 39-48, 2014.

Dr. A.K. Baliarsingh." A Low Rating Photovoltaic Fed Dstatcom for Harmonic Elimination and Power Factor Correction under Non-Sinusoidal Source" International Refereed Journal of Engineering and Science (IRJES), vol. 07, no. 04, 2018, pp. 04–14.